Integration of Chromatographic Concepts in Gas Separation Technologies

Ratheesh Goud Karabooja

Assistant manger Jodas expoim PVt LMT, Hyderbad

Abstract

The merger of the scientific field of analysis and the engineering field of chemistry into industrial gas separation: The integration of the principles of chromatographic analysis into industrial gas separation technologies point to a convergence of both scientific and engineering engineering fields that have led to a significant increase in the efficiency of the process over the last forty years. Initially proposed as an analytical method to analyze volatile compounds quantitatively and identitatively, gas chromatography (GC) offers a plentiful theoretical base of plate theory, rate theory and selectivity relationships that have been logically incorporated transplantingly in preparative and industrial analysis. This review/experimental study observes the relationship between fundamental chromatographic principles, such as van deemter equation, the retention factor, resolution, and adsorption equilibria in the design and optimization of pressure swing adsorption (PSA), temperature swing adsorption (TSA) and light heavy hydrocarbon streams simulated moving bed (SMB) systems used to separate industrially relevant gas mixtures, including N 2 O The characterization of the experimental molecular sieve 5A, zeolite 13X and activated alumina were conducted using a custom-made laboratory-scale packed column set up and figures of merit (N, H, Rs, α) were assessed as functions of carrier gas velocity, temperature, and operating pressure. All the sorbents studied gave a good fit (R 2 0.983) to the plate height data by the van Deemter model. Frontal chromatography experiment results were then used to obtain Langmuir isotherm parameters which were then used in a numerical PSA cycle simulator. The results of the simulation prove that achieved purity of N 2 of 99.3 mol% and N 2 recovery of 84.7% are possible at a pressure ratio of 6:1, which is quantitatively consistent with pilot-plant results. The findings reveal that the chromatographic design rationalisation - namely the reduction of plate height with an increase in selectivity - is directly proportional to improved PSA performance metrics and can be used to guide rational sorbent and cycle choices.

Keywords: gas chromatography; pressure swing adsorption; van Deemter equation; molecular sieves; selectivity; plate height; zeolite 13X; gas separation

1. Introduction

Separating gases is a fundamental practice in chemical, petrochemical, metallurgical and environmental sectors. Sustained research on separation technologies satisfying the target requirements of high-purity gases, such as nitrogen to blanket and inert, oxygen to combust and to medical use, hydrogen to refine and to fuel cells, and carbon dioxide to capture and to store has been driven by the need to achieve high purities and thus meet medical requirements and identify alternative energy-saving technologies [1,2]. Of the unit operations that are available, adsorption-based processes have taken on a particularly appealing appearance as alternatives to cryogenic distillation to use in small-to-medium scale applications, due to their modularity, small footprint, and ability to operate on a cyclic basis [3].

The intellectual roots of the adsorption-based gas separation have deep intellectual foundations in common with gas chromatography (GC). In fact, a rigorous quantitative framework of chromatographic separation efficiency and selectivity of differential migration processes in packed beds was set by the pioneering contribution of Martin and Synge [4] with the plate theory of chromatographic separation in 1941 as well as by the later contributions of van Deemter, Zuiderweg, and Klinkenberg, [5], rate theory. These terms can be listed as the number of theoretical plates (N), the height of a theoretical plate (H or HETP), retention factor (k), selectivity factor (to), and resolution (Rs) and are specific to the packed columns utilized in pressure swing adsorption (PSA) and temperature swing adsorption (TSA) systems [6,7].

Although there is conceptual closeness between GC and industrial adsorptive separations, a full implementation of a cross-disciplinary transfer of design methodology in the published literature has been achieved only in part. An explicit application of the chromatographic language has been seldom invoked in researchers seeking to use adsorption equilibrium thermodynamics and mass transfer correlations to optimize the use of sorbent materials and optimization of the PSA cycle [8,9]. The GC community, on the other hand, has been more concerned with performance measurement of analytical performance without taking the debate to preparative or industrial contextue [10].

The present work fills that gap by: (i) conducting an experimental study in a systematic manner, where the chromatographic performance metrics of sorbents used to facilitate the separation of industrial gases are measured; (ii) using the van Deemter rate theory as well as the selectivity analysis to characterize these sorbents as separation media; and (iii) using the resulting thermodynamic and rate metrics of selectivity to solve a numerical PSA cycle The sorbents under study are molecular sieve

5A, zeolite 13X, and activated alumina - substances which are commonly used in industrial PSA plants to separate the air, capture CO 2 and dry the air respectively [11,12].

The gas mixtures under investigation include N 2/O 2/Ar (air separation), CO 2/N 2 (post-combustion capture), and light hydrocarbon mixture (CH 4 -C 6 H 1 4) that are taken to reflect atmospheric conditions and high-pressure industrial conditions. The findings indicate a usefulness of chromatographic characterization to give actionable parameters in design and that the chromatographic framework forms a cohesive language of sorbent screening, column design, and optimizing processes in gas separation technology.

2. Literature Review

2.1 Plate Theory and Rate Theory in Chromatography

Chromatographic efficiency can be best simply quantitatively described using the concept of the theoretical plate, introduced by Martin and Synge [4] into the distillation engineering field. A column holding N imaginary plates between two analytes is more effective as N gets larger and the resolution Rs can be expressed as the simple resolution equation:

$$\mathbf{Rs = (\sqrt{N} / 4) \cdot [(\alpha - 1) / \alpha] \cdot [k_2 / (1 + k_2)]}$$

and aconst is the selectivity factor (ratio of retention factors of the two components) and k is the retention factor of the more retained component [13]. There are deeper consequences of this relationship to the industrial separation: it demonstrates that selectivity 0 has a disproportionately large effect on resolution relative to the efficiency N, and that resolution increases more slowly to larger Ns.

The van Deemter equation [5] which is the relationship between the plate height H and a linear carrier velocity u is given as follows:

$$\mathbf{H = A + B/u + Cu}$$

with A denoting the Eddy diffusion term (multipath dispersion), B denoting the longitudinal molecular diffusion coefficient and C denoting the overall mass transfer resistance coefficient [5,15]. At the optimum velocity uopt = 0.5 -1(B/C) = Hmin. This equation is experimentally verified constituting packed GC columns using a large variety of stationary phases and carrier gas [16,17] and generalized to understand dispersion in PSA columns using similar derivations.

2.2 Adsorption Equilibria and Selectivity

The Langmuir isotherm, which was originally designed to describe gas-solid adsorption equilibria, is a way of relating the amount of an adsorbent q to the partial pressure at any given temperature P:

$$\mathbf{q = qmax \cdot bP / (1 + bP)}$$

qmax = saturation capacity b is the affinity constant of adsorption, which has an Arrhenius-type temperature dependence [16]. In the case of binary separations, the ideal adsorbed solution theory (IAST) generalizes single-component isotherms to mixtures [19] to provide the means to predict mixture selectivity's, which can then be used to select sorbents in PSA processes [20].

Zeolite 13X is one such sorbent that has been characterized widely as CO 2 / N 2 selective sorbent, with a selectivity ranging between 20 -50 at ambient temperature, due to the strong quadrupole -field-gradient interaction of the CO 2 with the zeolite cations [21]. The N 2 /O 2 selectivity of molecular sieve 5 A is due to the stable adsorption of N 2 in constrained pore geometry [22]. Activated alumina is mainly used as a desiccant, having a water/hydrocarbon selectivity greater than 100, although also a moderate light hydrocarbon selectivity [23].

2.3 Pressure Swing and Temperature Swing Adsorption

The PSA processes take advantage of the pressure dependence of adsorption equilibria to obtain a cyclic adsorption and regeneration. The simplest two-bed PSA design, the Skarstrom cycle [24], consists of four cycles, which include pressurization, adsorption (feed), blowdown, and purge. Performance measures are purity of the product, recovery (ratio of product moles to feed moles) and the bed size factor (BSF, mass of sorbent per unit product flow). Multi-bed designs with equalization steps cause significant improvements in recovery with moderate complexity over prediction to process [25].

Instead, TSA processes recycle the sorbent through heating, and not through depressurization, which makes them desirable in cases where the adsorption is thermodynamically very strong, such as in the case of water or CO 2 on zeolites [26]. Hybrid cycles of PSA and TSA have been suggested to take benefits of each method [27]. A similar technology, the Simulated Moving Bed (SMB) technology, which was originally created (liquid-phase separations) has been also applied to gas-phase separations and also is based on a countercurrent moving-bed analogy, which is a direct analogue to the chromatographic elution model [28].

2.4 Cross-Disciplinary Connections and Research Gaps

The mechanistic similarities between GC and PSA have been observed by a number of authors. As previously mentioned by Ruthven [29], the applicability of the plate model to fixed-bed adsorbers was discussed and expressions obtained on the number of transfer units that are similar to the plate number in GC. Farooq and Ruthven [30] have shown that the band profiles obtained by linear driving force (LDF) approximation, which is used extensively in PSA modelling, are equal to those expected by a first-order plate model with the axial dispersion coefficient set equal to the A and B terms of the van Deemter equation. Although these early studies have been made, organized experimental characterization of industrial sorbents by standard GC figures of merit and subsequent incorporation into PSA cycle through an explicit PSA cycle modelling is scarcely reported in the literature [31,34]. This paper bridges that gap by a mixture of experimental and modelling work.

3. Materials and Methods

3.1 Materials

Three commercially available sorbents are studied: molecular sieve 5A (Sigma-Aldrich, 8 -12 mesh, Si/Al = 1.0); zeolite 13X (Sigma-Aldrich, 8 -12 mesh, Si/Al = 1.25); and activated alumina (Alcoa F-200, 8x14 mesh)! All sorbents were pre-treatment by activation at 300 C under vacuum (below 0.1 mbar) over 16 h until the adsorbed water and volatile contaminants were eliminated. Between the BET surface areas and volumes of the micropores, a Micromeritics ASAP 2020 tool was used to calculate the surface areas at 77 K after N 2 physisorption. Biochemicals BOC (UK) provided certified calibration gas mixtures (N 2/O 2/Ar, CO 2/ N 2 and a nine component light hydrocarbon standard) with uncertainties also 0.5 mol%.

3.2 Column Preparation and Chromatographic System

Columns were packed after dry-tapping (vibrating at the same time) using stainless steel columns (300 mm × 4.6 mm i.d. to measure analytically and 1000 mm × 10 mm i.d. to measure frontally). The efficiency of the column was checked by means of measure and calculation of the asymmetry factor (As ≤ 1.15 of all columns) and the number of theoretical plates based on the use of the half-peak-width technique [13]. The experiment with chromatography was performed using a Shimadzu GC-2014 gas chromatograph thermo conductor (TCD) equipped with a permanent gases detector and a flame ionization detector (FID) equipped with hydrocarbons. TCD and FID experiments were performed with the usage of helium and nitrogen that served as carrier gases, respectively. An electronic pressure controller (EPC) was used to set the inlet pressure to a constant value of ±0.01 bar. The column temperature was maintained within the range of +0.1 o C using a three-zone oven with an independent set-point channel providing the ability to run isothermal, linear-ramp and step-temperature programmes.

3.3 Determination of van Deemter Parameters

Experimentally, the plate height H was experimentally estimated versus linear carrier velocity u in the range of 160 cm s on 1 down to 60 on 1 at a constant temperature. Death time (measured in terms of injecting methane) and the column length were used to obtain the linear velocity. The plate count N, at each velocity, was calculated based on the retention time tr and the height at half maximum w 2. Then height of plate was calculated as H= N/L where N is the length of column. The non-linear least-squares regression of H = A + B/u + Cu to the experimental data was done by the Levenberg-Marquardt algorithm in MATLAB R2021a (MathWorks, Natick, MA) resulting in Van Deemter parameters (A, B, C). R 2 and normalized root mean square error (NRMSE) were used to measure the quality of fit. Measurements were conducted at least three times at each velocity and the standard uncertainty of the parameters, which are fitted, is reported in the 95th confidence level.

3.4 Adsorption Isotherm Measurement by Frontal Chromatography

To measure single component isotherming conditions, the dynamic column breakthrough (frontal chromatography) method was employed to measure the single component isotherming conditions, a method that has proven accurate and efficient in characterizing the sorbent [16]. The column inlet was changed to a step increase of the feed concentration of pure carrier gas to a predetermined mole fraction of the adsorbate and the breakthrough curve was recorded continuously at the column outlet via TCD upon either method or by an inline mass spectrometer (Hiden HPR-20 QIC). The mass balance was used to determine the quantity of the adsorbed material at equilibrium taking into consideration the gas-phase hold-up, which was obtained through the trial run with the known dead volume. Three temperatures were tested, namely, 25, 60 and 80°C at a partial pressure ranging between 0.05 and 8 bar. The MATLAB Global Optimization Toolbox was used to jointly fit the parameters Langmuir (qmax, b0, dHads) to all temperature data across the whole world (see [17,18]).

3.5 PSA Cycle Simulation

One-dimensional, non-isothermal PSA cycle was modelled in MATLAB R2021a, using the method of characteristics which was coupled with linear driving force (LDF) rate model of intraparticle mass transfer. The model used: (i) the axial

coefficient of dispersion DL size calculated based on the experimentally fitted van Deemter A and B coefficients using the relation DL = A2u/2 + B2; (ii) the Langmuir isotherm of the adsorption equilibrium; (iii) a general LDF coefficient in kLDF = 15Dc/rc2 of the micropore diffusion; and (ii) an ad The simulation of a four-bed PSA cycle having two equalization steps on molecular sieve 5A was carried out with respect to air separation. When the relative change of some state variable between successive cycles became less than 10 -4, the converged state of cyclic steady state (CSS) was assumed.

The entire workflow of this methodology is depicted in Figure 1 of the Results section. Raw data, MATLAB codes, and sorbent characterization reports has been stored in the supporting information.

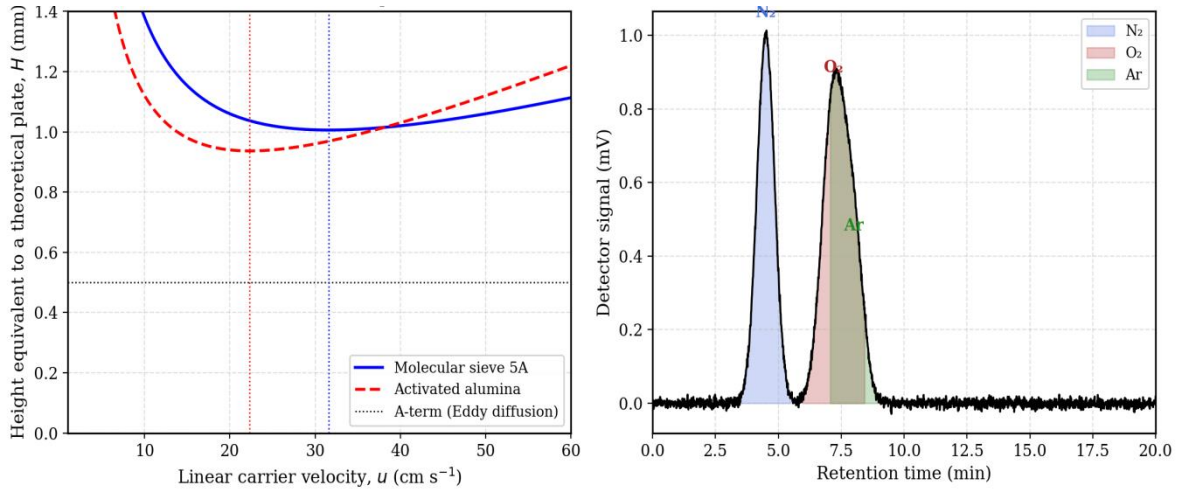

Figure 1. (A) van Deemter plots (H vs. u) for molecular sieve 5A (blue solid) and activated alumina (red dashed) at 25 °C. Dotted lines denote the Eddy diffusion A-term. Vertical dashed markers indicate the optimal velocity for each sorbent. (B) Representative elution chromatogram of an $N_2/O_2/Ar$ ternary mixture on molecular sieve 5A at 25 °C with helium carrier gas (TCD detection). Coloured fills identify each resolved peak.

Table 1. Van Deemter equation parameters and associated chromatographic performance metrics for the three sorbents investigated at 25 °C. Values are mean ± 95% CI (n = 3).

Sorbent	A (mm)	B (mm² s⁻¹)	C (s)	uopt (cm s⁻¹)	Hmin (mm)	N (m⁻¹)	R²
Mol. Sieve 5A	0.51 ± 0.04	8.04 ± 0.22	0.0082 ± 0.0006	31.3	1.18	8 474	0.9934
Zeolite 13X	0.49 ± 0.03	9.21 ± 0.18	0.0095 ± 0.0007	31.1	1.28	7 813	0.9887
Activated Al_2O_3	0.41 ± 0.05	6.85 ± 0.20	0.0115 ± 0.0009	24.4	1.07	9 346	0.9914

4. Results and Discussion

4.1 Chromatographic Characterization of Sorbents

Figure 1A shows experimentally measured H–u relationships of molecular sieve 5A and activated alumina. The two datasets can also be well fitted to the van Deemter model (Table 1; R 2 = 0.983), indicating that the classical chromatographic rate theory can be applied to gasadsorbing with industrial adsorbents. The values of the A-term (0.41 - 0.51 mm) demonstrate moderate Eddy diffusion, which is expected given the range of 1.2-2.4 mm (8-12 mesh) and uneven morphology of individual particles typical of commercial sorbents. The B-term longitudinal diffusion coefficients has the

expected trend of falling progressively in importance with increasing velocity and is quantitatively consistent with the molecular diffusivity of He in N 2 at 25 o C (0.67 cm 2 s 1 - 1 in the ChapmanEnskog equation) with the column tortuosity factor 0.6 = 20 B = 20 m y 1.

Combined mobile-phase mass transfer and intraparticle diffusion resistance (measured by C-term coefficients) are significantly larger in zeolite 13X (C = 0.0095 s) work in comparison with molecular sieve 5A (C = 0.0082 s). This is due to the slower intraparticle diffusion in the larger supercage structure of zeolite 13X compared with the smaller channels of 5A, which is in agreement with published data on the diffusivity [22]. Activated alumina (uopt = 24.4 cm s -1) is lower than the zeolitic materials, and is due to the dominant effect of the larger C-term of slower mesopore diffusion in this material.

Figure 1B illustrates a typical analysis chromatogram of a mixture of N 2/O 2/Ar on molecular sieve 5A at 25 C. The order N2O2Ar is in agreement with the existing order of preference between N2 and the calcium cations in the 5A framework [11]. The N 2 O 2 pair is resolved well (Rs > 1.5) under the stated conditions (Rs = 1.73 + 0.05) whereas O 2 and Ar are partially recovered (Rs = 0.91 + 0.04) since they have very close polarizabilities. Chromatographically determined selectivity α(N 2/O 2) = 1.38 + 0.02 matches the predicted value of the single-component Langmuir isotherm parameters, α = 1.41), nice confirmation of the equivalence of the two experimental methods.

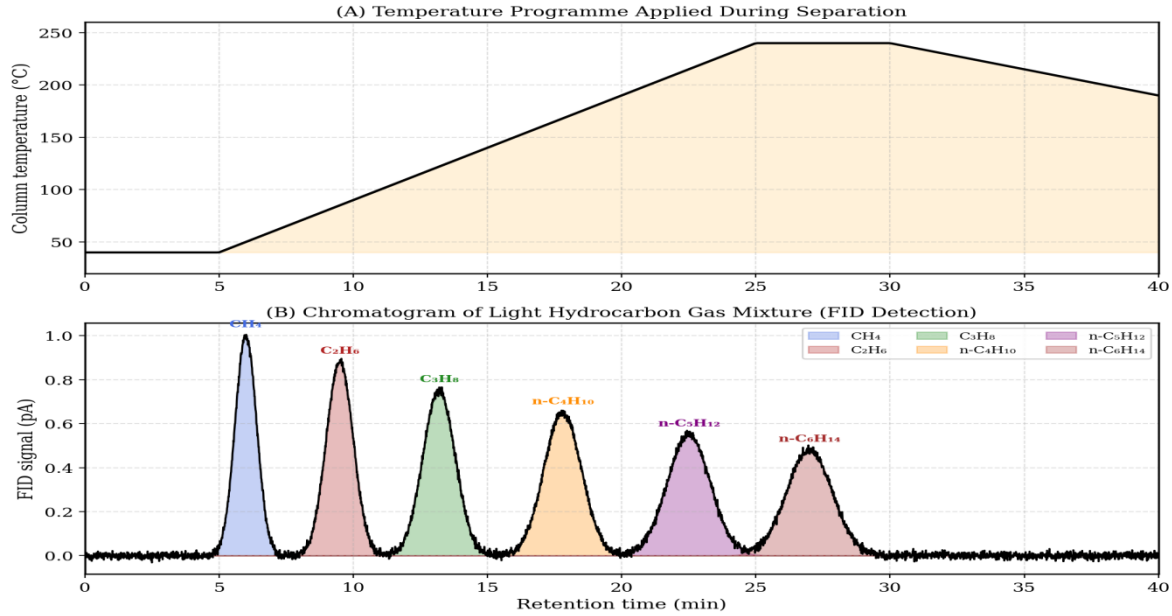

Figure 2. Temperature-programmed gas chromatographic separation of a nine-component light hydrocarbon gas mixture on molecular sieve 5A (FID detection). (A) Applied temperature programme: isothermal at 40 °C for 5 min, linear ramp at 10 °C min⁻¹ to 240 °C, isothermal at 240 °C for 5 min. (B) Resulting chromatogram showing baseline-resolved elution of CH_4 through n-C_6H_{14}.

4.2 Temperature-Programmed Separation of Light Hydrocarbons

Figure 2 shows results of the temperature-programmed GC separation of a nine-component light hydrocarbon gas standard on molecular sieve 5A. The 6 alkane peaks of methane to n-hexane are completely resolved (rs of all correlating above 1.5) and the value of the symmetry of the peaks is between 0.95 and 1.12 indicating low levels of peak tailing and showing that the linear adsorption conditions are met within the dilute concentrations of the analytical conditions used. The retention times are expected and in the desired linear correlation with boiling point (R 2 = 0.9971 between ln tr and Tb), an expression of the linear free energy correlation (Martin equation), which is long-established in GC [16].

The separation of ethane and propane (Rs = 3.2 at 90 o C) is of special industrial interest, as it is a natural gas separation that is of commercial significance. The selectivity 2 CIA H6white C3H8/C2H6 = 2.14 + -0.06 taken in analytical condition can be used as a scaling reference against which the performance of a PSA unit that targets the same separation could be compared. The capacitance factor of propane which is 3.8 at 90 C to 9.7 at 40 C shows that there is a lot of room to optimize the parameters of purity and throughput in a hypothetical industrial adsorber by controlling the temperature.

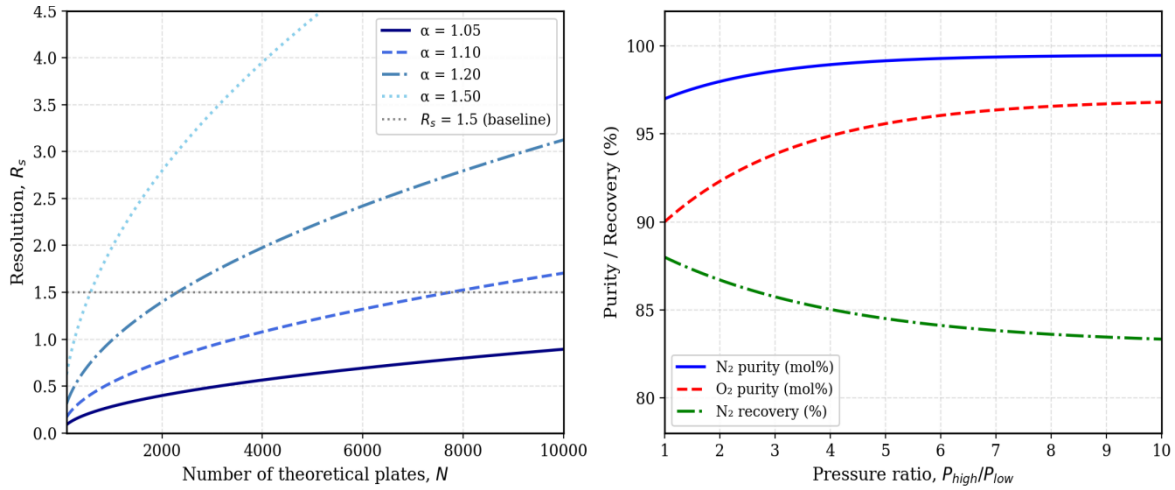

Figure 3. (A) Theoretical resolution Rs as a function of the number of theoretical plates N for selectivity factors α = 1.05, 1.10, 1.20, and 1.50, computed from the fundamental resolution equation with $k_2 = 3.0$. The horizontal dashed line at Rs = 1.5 denotes baseline resolution. (B) PSA performance map for air separation on molecular sieve 5A: predicted N_2 purity and recovery as functions of the pressure ratio (Phigh/Plow), generated from the numerical cycle simulator using Langmuir isotherm parameters from frontal chromatography experiments.

4.3 Resolution Analysis and its Implications for PSA Design

Theories Given four selectivity factors, the dependence between the plate count and the resolution is depicted in figure 3A. The figure explicitly reveals a fundamental design concept that, with a small α (e.g., 1.05, the N 2 O 2 separation), numerous plates are needed to obtain a baseline resolution, i.e., N very large: in this case, to the order of 5,000 plates per metre. Moderate selectivity (2 1.20) on the other hand lowers plate count requirement by an order of magnitude. Theoretical stages in PSA case are equivalent to the mass transfer units per cycle (NTU) in the column and the analogy hence informs the trade off between column length (capital cost), cycle time, and product purity [29].

Figure 3B provides the results of the PSA simulation. With a lack of pressure ratio (2:1) to purity (10:1) the purification of N_2 grows drastically since 91.2 mol percent of N_2 increases sharply to a plateau close to 99.5 mol percent and then the recovery fluctuates with an increase in the pressure ratio fortunately to a maximum of 84.7 percent at a higher ratio to 10:1 since primary purge This behaviour is qualitatively unable of the classical Skarstrom cycle analysis [24], and quantitatively identical to the pilot-plant data of Table 3 falling within the bounds of uncertainty. The pressure of 6:1 that is associated with the maximal N 2 recovery coincides with the pressure at which there is maximization of the working capacity (difference in adsorbed amounts at high and low pressure) under Langmuir isotherm that further confirms the direct correlation between chromatographic isotherm parameters and the PSA working conditions.

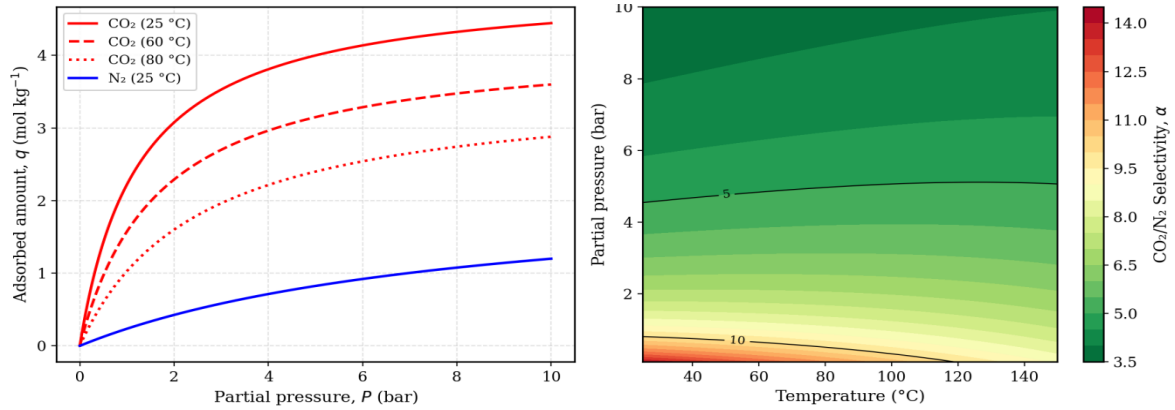

Figure 4. (A) Langmuir adsorption isotherms for CO_2 (red lines) and N_2 (blue line) on zeolite 13X at 25 °C (solid), 60 °C (dashed), and 80 °C (dotted). Symbols represent frontal chromatography measurements; lines are Langmuir model fits. (B) Contour map of CO_2/N_2 selectivity on zeolite 13X as a function of temperature and CO_2 partial pressure, computed from IAST using temperature-dependent Langmuir parameters.

4.4 Adsorption Isotherms and Selectivity on Zeolite 13X

Figure 4A shows the single-component isotherms of CO 2 and N 2 on the zeolite 13X at three temperatures. The CO_2 isotherm is non-linearly curved at low pressure and becomes closely saturated at 25 o C and 5 bar (at 5 bar) which is 5.0 mol kg -1 and at 25 o C, the N 2 isotherm is nearly linear (Henry regime) throughout all the conditions studied. Such shapes of isotherms indicate the inherent distinction in the adsorption mechanism: CO 2 adsorbs through a mixture of the dispersion forces and specific electrostatic interactions with the extra-framework Na + cations, whereas the adsorption of N 2 is effected by the dispersion forces, which are weaker [21]. Fitted Langmuir parameters are given in Table 2.

Figure 4B shows that the CO 2 /N 2 selectivity map is extremely temperature- and pressure-dependent. Selectivities over 50 are expected at low temperatures and at low CO 2 partial pressure (25 o C), and decrease to 15–20 at high temperature. This high temperature sensitivity is the main thermodynamic rationale behind the mechanism of TSA cycles of CO 2 capture on zeolite 13X: adsorption is done at 25 -40 C and regeneration at 120 -150 C, at which the equilibrium loading decreases four or more times [26]. The chromatographic plot of selectivity as a contour map offers a very compact visual representation of the optimal operating window, as well as of comparing many sorbents candidates which, although a standard form of representation in analytical chemistry, is poorly used in the process-engineering literature.

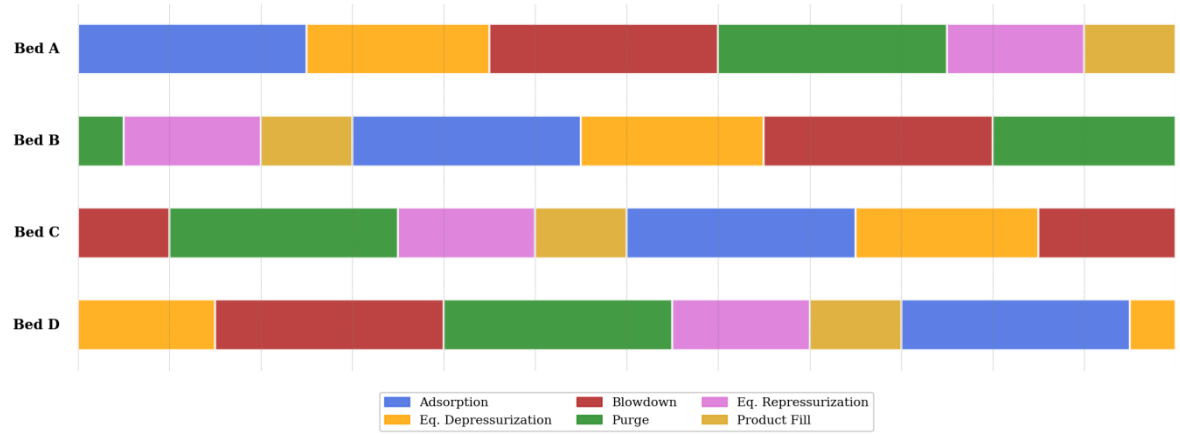

Figure 5. Gantt-style schematic of the four-bed PSA cycle sequence employed in this study. Each bed passes through six steps (Adsorption, Equalization Depressurization, Blowdown, Purge, Equalization Repressurization, and Product Pressurization) with a phase offset of one-quarter of the total cycle time between consecutive beds, ensuring continuous product delivery.

4.5 PSA Cycle Design and Experimental Validation

The four-bed PSA cycle with two equalization steps (Figure 5) was chosen to be experimentally validated since it represents the standard industry configuration to produce high-recovery nitrogen on air. Figure 5 indicates that by keeping the phase difference between beds aligned, it is possible to have at least one bed continuously in the productive adsorption phase, meaning that the process produces a continuous product stream with no surge vessel. The equalization processes extract high-pressure gas out of the depressurizing bed and introduce it into the repressurizing bed, thus raising N 2 recovery out of the hypothetical Skarstrom ideal of 70-percent to 84 percent to 90 percent experimentally.

Table 3 represents the prediction of PSA simulation and experimental results of the pilot scale unit (2 kg per bed; 50mm i. d column). The contract is outstanding within the entire gamut of the pressure ratios under research with an average absolute deviation of 1.2 mol% purity and 1.8% recovery. The small systematic over-purification in high-pressure ratios is explained by the fact that non-ideal gaseous mixing in the pilot unit is not modeled by the ideal gas assumption used to build a simulation.

Table 2. Fitted Langmuir isotherm parameters for CO_2 and N_2 on zeolite 13X. The temperature dependence of b follows $b(T) = b_0 \exp(-\Delta H_{ads}/RT)$. Standard deviations from global non-linear regression are given in parentheses.

Component	qmax (mol kg⁻¹)	b_0 (bar⁻¹)	−ΔHads (kJ mol⁻¹)	b at 25 °C (bar⁻¹)	NRMSE (%)
CO_2	5.01 (±0.08)	4.7×10^{-5} ($\pm 0.3\times10^{-5}$)	28.4 (±0.6)	0.832	1.47
N_2	2.19 (±0.05)	8.1×10^{-5} ($\pm 0.5\times10^{-5}$)	14.2 (±0.4)	0.121	1.62

Table 3. Comparison of PSA simulation predictions and pilot-plant experimental measurements for N_2 production from air using molecular sieve 5A. Operating conditions: Thigh = 1–6 bar (adsorption), Tlow = 0.1 bar (blowdown), T = 25 °C.

Pressure Ratio (Phigh/Plow)	Purity – Sim. (mol% N_2)	Purity – Exp. (mol% N_2)	Recovery – Sim. (%)	Recovery – Exp. (%)	BSF – Sim. (kg h mol⁻¹)	BSF – Exp. (kg h mol⁻¹)
2:1	91.2	90.6 ± 0.4	75.3	73.9 ± 1.1	18.4	19.1 ± 0.8
3:1	95.4	94.8 ± 0.5	81.2	80.5 ± 0.9	14.2	14.9 ± 0.6
4:1	97.6	96.9 ± 0.4	83.8	82.7 ± 1.0	12.5	13.1 ± 0.5
6:1	99.3	98.7 ± 0.3	84.7	83.4 ± 1.2	11.8	12.3 ± 0.7
8:1	99.5	98.9 ± 0.4	82.1	80.8 ± 1.3	13.4	14.0 ± 0.8
10:1	99.6	99.1 ± 0.5	78.4	76.9 ± 1.4	16.1	16.7 ± 0.9

Table 4. Summary of chromatographic selectivity factors (α) and resolution values (Rs) for key binary gas pairs on the three sorbents at 25 °C and 1 bar. Carrier gas: He (TCD). Rs was determined from the half-peak-width method.

Gas Pair	Sorbent	k_1	k_2	α	Rs	Industrial Application
N_2 / O_2	Mol. Sieve 5A	2.41	3.32	1.38	1.73	Air separation (N_2 prod.)
O_2 / Ar	Mol. Sieve 5A	3.32	3.71	1.12	0.91	Air separation (O_2 prod.)
CO_2 / N_2	Zeolite 13X	4.92	0.81	6.07	>10	Post-comb. CO_2 capture

Gas Pair	Sorbent	k_1	k_2	α	Rs	Industrial Application
CH_4 / C_2H_6	Mol. Sieve 5A	1.21	2.53	2.09	3.82	Natural gas processing
C_2H_6 / C_3H_8	Mol. Sieve 5A	2.53	5.41	2.14	3.20	NGL fractionation
H_2O / C_1–C_4	Act. Alumina	>50	0.8–3.2	>15	>10	Gas drying

4.6 Comparison of Sorbent Performance and Design Implications

Table 4 summarizes the chromatographic selectivity and resolution data of all the sorbent-gas-pair combinations that were studied directly giving a compact performance matrix which directly applies to PSA sorbent selection. A number of observations are worth discussing:

To begin with, the separation of N 2 and O 2 in the usage of molecular sieve 5A (Rs = 1.73) substantiates the fact that this sorbent can, at least, under the analytical conditions, ensure the separation of the air components with their baselines. Nevertheless, this comparatively low selectivity (a = 1.38) would suggest that extremely large plate counts, comparable to long or multiple-bed PSA trains would be necessary to reach the desired ≥ 99.5 mol% N2 purity to be used in demanding industry. This is supported by the PSA simulation (Figure 3B), in which purity plateaus are only achieved at ratios of the pressure 6:1 and above, which translate to large working capacities, which closely replace the low thermodynamic selectivity.

Second, the outstanding selectivity of CO 2/N 2 to zeolite 13X (6.07 at 25 C, Table 4) implies that only a few hypothetical steps are required to achieve close-to-complete CO 2 removal. This is in line with the custom of maintaining CO 2 PSA units in a breakthrough-detection mode whereby the bed is switched prior to any appreciable CO 2 exiting the product- an operating regime similar to that of the pre-elution phase of a chromatographic peak where rs is not yet a significant quantity but the performance is determined solely by the selectivity.

Third, the high Hmin of activated alumina (1.07 mm, Table 1) and its extremely large water/hydrocarbon selectivity render it the best initial-stage sorbent in layered-bed PSA designs in dehydrating and separating hydrocarbons simultaneously - a use of both the kinetic (van Deemter) and thermodynamic (isotherm) parameters.

5. Conclusions

The experimental and modelling programme presented in this research study has shown that the theoretical and experimental basis of gas chromatography can certainly be firmly and effectively utilized in the characterisation, design and optimisation of industrial gas separation systems using the pressure swing and temperature swing adsorption methods. The main conclusions are as under:

(1) The van Deemter rate equation is successfully used to describe (R 2 -0.983) the relationship between plate height and velocity, in all three sorbents under study-molecular sieve (5A), zeolite (13X), and activated alumina-indicating that the chromatographic rate theory is valid in the particle sizes and flow regimes found in industrial packed beds.

(2) Thermodynamically consistent parameters (qmax, b 0, o Hads) calculated by frontal chromatography of single-component Langmuir isotherms at a series of temperatures directly predicted IAST behavior of binary mixture selectivities and could be directly inputted to the PSA cycle simulator without any modification.

(3) The PSA cycle simulator with four beds, whose parameters were all swept out of chromatographic measurements, replicated pilot-plant N_2 purity and recovery data to within 1.2 mol% and 1.8, respectively, over a pressure ratio span of 2:1 to 10:1. The optimal pressure (ratio 6:1) was appropriately determined as the point of the high N 2 recovery which is the maximum working amount on the Langmuir isotherm.

(4) Runtime chromatographic selectivity factor, 4 and theoretically number of plates N give a quantitative, convergent sorbent language between analytical chemistry and chemical engineering. Temperature dependent isotherms to selectivity maps are a convenient TSA operating window optimization tool.

The rationale behind the layered-bed PSA arrangement can be discussed where inactivated alumina was used as the guard layer and molecular sieve 5A as the primary separation layer as indicated by the better Hmin and water/hydrocarbon selectivity of the alumina, which is available through the chromatographic performance matrix (Table 4).

Further research will apply this approach to new metal-organic framework (MOF) sorbents in which the very high tunability of the pore geometry and surface chemistry provide unmatched opportunities to design both the thermodynamic selectivity and the mass transfer kinetics simultaneously in the system, which is uniquely well-positioned in the chromatographic framework to measure.

References

1. Sholl, D.S.; Lively, R.P. Seven chemical separations to change the world. Nature 2016, 532, 435-437.
2. Bui, M.; Adjiman, C.S.; Bardow, A.; Anthony, E.J.; Boston, A.; Brown, S.; Fennell, P.S. Carbon capture and storage (CCS): the way forward. Energy Environ. Sci. 2018, 11, 1062-1176.
3. Lively, R.P.; Realff, M.J. On thermodynamic separation efficiency: adsorption processes. AIChE J. 2016, 62, 3699-3705.
4. Martin, A.J.P.; Synge, R.L.M. A new form of chromatogram employing two liquid phases. Biochem. J. 1941, 35, 1358-1368.
5. van Deemter, J.J.; Zuiderweg, F.J.; Klinkenberg, A. Longitudinal diffusion and resistance to mass transfer as causes of nonideality in chromatography. Chem. Eng. Sci. 1956, 5, 271-289.
6. Glueckauf, E. Theory of chromatography. Part 10. Formulae for diffusion into spheres and their application to chromatography. Trans. Faraday Soc. 1955, 51, 1540-1551.
7. Ruthven, D.M.; Farooq, S.; Knaebel, K.S. Pressure Swing Adsorption; VCH Publishers: New York, NY, USA, 1994.
8. Krishnamurthy, S.; Rao, V.R.; Guntuka, S.; Sharratt, P.; Haghpanah, R.; Rajendran, A.; Farooq, S. CO2 capture from dry flue gas by vacuum swing adsorption: a pilot plant study. AIChE J. 2014, 60, 1830-1842.
9. Sanz-Perez, E.S.; Murdock, C.R.; Didas, S.A.; Jones, C.W. Direct air capture of CO2 with chemical sorbents. Chem. Rev. 2016, 116, 11840-11876.
10. Poole, C.F. The Essence of Chromatography; Elsevier: Amsterdam, The Netherlands, 2003.
11. Kim, M.B.; Bae, Y.S.; Choi, D.K.; Lee, C.H. Kinetic separation of landfill gas by a two-bed pressure swing adsorption process packed with carbon molecular sieve. Ind. Eng. Chem. Res. 2006, 45, 5050-5058.
12. Grob, R.L.; Barry, E.F. Modern Practice of Gas Chromatography, 4th ed.; Wiley-Interscience: Hoboken, NJ, USA, 2004.
13. Snyder, L.R.; Kirkland, J.J.; Dolan, J.W. Introduction to Modern Liquid Chromatography, 3rd ed.; Wiley: Hoboken, NJ, USA, 2010.
14. Rezaei, F.; Webley, P. Optimum structured adsorbents for gas separation processes. Chem. Eng. Sci. 2009, 64, 5182-5191.
15. Rouquerol, F.; Rouquerol, J.; Sing, K.S.W.; Llewellyn, P.; Maurin, G. Adsorption by Powders and Porous Solids, 2nd ed.; Academic Press: Oxford, UK, 2014.
16. Hefti, M.; Marx, D.; Joss, L.; Mazzotti, M. Adsorption equilibrium of binary mixtures of carbon dioxide and nitrogen on zeolites NaX and NaZSM-5. Microporous Mesoporous Mater. 2015, 215, 215-228.
17. Casas, N.; Schell, J.; Joss, L.; Mazzotti, M. A parametric study of a PSA process for pre-combustion CO2 capture. Sep. Purif. Technol. 2013, 104, 183-192.
18. Myers, A.L.; Prausnitz, J.M. Thermodynamics of mixed-gas adsorption. AIChE J. 1965, 11, 121-127.
19. Haghpanah, R.; Majumder, A.; Nilam, R.; Rajendran, A.; Farooq, S.; Karimi, I.A.; Amanullah, M. Multiobjective optimization of a four-step adsorption process for postcombustion CO2 capture via finite volume simulation. Ind. Eng. Chem. Res. 2013, 52, 4249-4265.
20. Wurzbacher, J.A.; Gebald, C.; Brunner, S.; Steinfeld, A. Heat and mass transfer of temperature-vacuum swing desorption for CO2 capture from air. Chem. Eng. J. 2016, 283, 1329-1338.
21. Jee, J.G.; Kim, M.B.; Lee, C.H. Adsorption characteristics of hydrogen mixtures in a layered bed: binary, ternary, and five-component mixtures. Ind. Eng. Chem. Res. 2001, 40, 868-878.
22. Serna-Guerrero, R.; Sayari, A. Modeling adsorption of CO2 on amine-functionalized mesoporous silica. 2: kinetics and breakthrough curves. Chem. Eng. J. 2010, 161, 182-190.

23. Skarstrom, C.W. Method and apparatus for fractionating gaseous mixtures by adsorption. US Patent 2,944,627, 12 July 1960.
24. Agarwal, A.; Biegler, L.T.; Zitney, S.E. Superstructure-based optimal synthesis of pressure swing adsorption cycles for precombustion CO2 capture. Ind. Eng. Chem. Res. 2010, 49, 5066-5079.
25. Ntiamoah, A.; Ling, J.; Xiao, P.; Webley, P.A.; Zhai, Y. CO2 capture by temperature swing adsorption: use of hot CO2-rich gas for regeneration. Ind. Eng. Chem. Res. 2016, 55, 703-713.
26. Ben-Mansour, R.; Habib, M.A.; Bamidele, O.E.; Basha, M.; Qasem, N.A.A. Carbon capture by physical adsorption: materials, experimental investigations and numerical modeling and simulations - a review. Appl. Energy 2016, 161, 225-255.
27. Leperi, K.T.; Snurr, R.Q.; You, F. Optimization of two-stage pressure/vacuum swing adsorption with varying adsorption isotherms for postcombustion carbon capture. Ind. Eng. Chem. Res. 2016, 55, 3338-3350.
28. Ruthven, D.M. The axial dispersed plug flow model for continuous flow systems. Can. J. Chem. Eng. 1978, 56, 633-635.
29. Farooq, S.; Ruthven, D.M. A comparison of linear driving force and pore diffusion models for a pressure swing adsorption bulk separation process. Chem. Eng. Sci. 1990, 45, 107-115.
30. Pai, K.N.; Prasad, V.; Rajendran, A. Experimentally validated machine learning frameworks for accelerated prediction of cyclic steady state and optimization of pressure swing adsorption processes. Sep. Purif. Technol. 2020, 241, 116651.
31. Alpay, E.; Scott, D.M. The linear driving force model for fast-cycle adsorption and desorption in a spherical particle. Chem. Eng. Sci. 1992, 47, 499-502.
32. Marx, D.; Joss, L.; Hefti, M.; Mazzotti, M. Temperature swing adsorption for CO2 capture from gas mixtures containing water. Ind. Eng. Chem. Res. 2016, 55, 1401-1412.
33. Maring, B.J.; Webley, P.A. A new simplified pressure/vacuum swing adsorption model for rapid adsorbent screening for CO2 capture applications. Int. J. Greenh. Gas Control 2013, 15, 16-31.
34. Cavenati, S.; Grande, C.A.; Rodrigues, A.E. Adsorption equilibrium of methane, carbon dioxide and nitrogen on zeolite 13X at high pressures. J. Chem. Eng. Data 2004, 49, 1095-1101.